Article citation info:
Fouellefack LD, Feukeu EA, Mbuyu S, Mokhotjwa D. Internal combustion modelling for aerospace applications. Combustion Engines. 0000;XXX(X):xx-xx. https://doi.org/10.19206/CE-220545

Lionel Dongmo FOUELLEFACK
Etienne Alain FEUKEU
Sumbwanyambe MBUYU
Dhlamini MOKHOTJWA

Combustion Engines
Polish Scientific Society of Combustion Engines

Internal combustion modelling for aerospace applications

ARTICLE INFO

Received: 6 February 2026
Revised: 30 March 2026
Accepted: 10 April 2026
Available online: 12 June 2026

A model of an internal combustion engine (ICE) was created in Simulink and could be used as part of the drive component of the propulsion system during the development stage of an unmanned aerial vehicle (UAV)/Aircraft. The model can predict the engine power, engine torque, engine brake-specific fuel consumption, and engine fuel flow of an ICE for a given engine throttle, atmospheric pressure, rotational speed, temperature, and altitude at which the UAV is flying. Results from the model were compared with those of previous researchers reported in the literature. The engine power, torque, fuel flow, and brake-specific fuel consumption curves from simulations were found to be in good agreement with those obtained experimentally by previous researchers.

Key words: *unmanned aerial vehicle, internal combustion engine, brake specific fuel consumption, fuel flow, manifold air pressure*

1. Introduction

An Internal Combustion Engine (ICE) is a crucial driving component of a UAV as it provides the thrust and power that can be used to propel a UAV in flight. In an ICE, the air from the combustion chamber is mixed with fuel, which is ignited to produce the power and torque that can be used to drive the propeller in flight. To estimate the power and torque produced by a UAV, a working model is very important during the early development stages of an aircraft, as it can help the engineer predict the power and thrust requirements of the ICE to drive the UAV's propeller in flight. One of the main challenges in designing an ICE for a UAV application is creating a model that can simulate the ICE at the various temperatures and altitudes at which the UAV is flying. Previous researchers have attempted to develop an engine model for simulation, which was experimentally validated. The models developed by the researchers were used as drive components for Hybrid Electric Vehicles [1, 19], Hybrid track vehicles [18], and ship hull propulsion for marine applications [21]. Stewart et al. [19] presented an engine simulation model of an ICE for a series hybrid electric vehicle. The engine performance curves obtained from the model were validated with experimental results of a V6 Ford Duratec gasoline engine. A similar study was also conducted by Al-Atabi et al. [1], in which experiments were performed to determine the optimal performance of an ICE for a hybrid power unit of a series-hybrid electric vehicle. The engine performance curves obtained from the experiment showed that the ICE performed at its optimum at an engine speed between 2000 – 2500 rpm and a charging load of 1 kW. Another study was conducted by Shanmuganathan et al. [18], who developed a dynamic model of an ICE as a drive component for a hybrid track vehicle in Simulink. The author generated torque and power curves, which were validated using test data for a 1100 hp, 800 kW generator. Also, Magdas et al. [14] developed an engine simulation model of an ICE using the Loftus Engine simulation software to predict its behavior. Using the simulation software, the author generated torque and brake power curves for the modeled ICE. In addition, Tadros et al. [21] carried out the numerical simulation of a 2-stroke marine diesel engine as a drive component for the propulsion system of a ship hull. The model results were then compared with experimental data from a real engine, yielding a good match. A lot of related work was also carried out by previous researchers, where they developed engine models for heavy-duty diesel engine trucks [4], automobile vehicle applications [16], and motorsports cars [8]. Another challenge posed by previous researchers was to create an ICE model that could be matched with a turbocharger to increase boost power. Many researchers have attempted to resolve this issue by developing an engine model that can be matched with a turbocharger to increase boost power [3, 5, 6, 9]. For example, Chen et al. [5] developed a simulation model to increase the power output of a 9-L Tier IV turbocharged diesel engine using GT–Power. The authors showed that their engine simulations accurately predict actual engine performance curves, resulting in a 1.5% reduction in BSFC and a 0.4% increase in torque. Hameur et al. [9] developed an engine simulation model to match a turbocharger with an ICE. Through simulations, the authors generated engine performance curves which were validated with results from Richard wave simulations. Chen et al. [6] developed a simulation model of a gasoline engine to perform a turbocharger match to boost its power and torque using GT–Power software. Through simulation, the author obtained torque, power, and BSFC curves for the gasoline engine, resulting in about a 4% reduction in fuel consumption. Ammad Ud Din et al. [3] developed an ICE engine simulation model to match a turbocharger and validated it using engine test data in GT-POWER. The authors obtain engine torque and BSFC curves, resulting in a 5.26% increase in engine torque and a 4.31% decrease in BSFC. Also, the engine performance curves obtained from the model were found to be in close agreement with experimental data by 5%. Very little research was carried out on modeling studies related to UAV Combustion engines. Some contributions are highlighted in this paper. Kravchenko et al. [13] developed a fuel injection system to boost power and reduce fuel con-

sumption in a 2-stroke engine used in a small UAV. Through simulations, the author increased the boost power and UAV flight duration by using an electronic fuel injection system. Kang et al. [12] developed a turbocharger system to provide pressure boost for a High-Altitude Long Endurance UAV powered by an ICE, thereby reducing the engine's sensitivity to altitude. Yixuan et al. [23] proposed an air-fueled Ratio Controlled strategy to boost the power of a fuel-powered UAV. Through simulation, he boosted the UAV engines power from 9% to 33%. Wróblewski et al. [22] designed an experimental test stand for thrust matching across various propeller sizes and for detecting anti-wear coatings in 2-stroke piston engines of small aircraft. However, no attempt to create an ICE model for a UAV has been reported in the literature surveyed. This paper thus provides a unique modelling approach for an ICE that could be used as a drive component of a UAV by estimating the power thrust, BSFC, and Fuel flow of the ICE at various temperatures, pressures, and altitudes during the flight of the UAV.

2. Methodology

The ICE was modelled in the MATLAB-Simulink environment using engine data from [11]. The developed ICE model was applied to UAV combustion, such as the Aersonde UAV, which uses a 22 ccm Avgas 1 kW single-cylinder port fuel injection combustion engine [20]. The input parameters to the model are the engine throttle, engine atmospheric pressure, engine rotational speed, and temperature at the UAV's reference altitude, as shown in the boxes in Fig. 1. The model determines the ICE power, ICE Torque, Brake Specific Fuel Consumption, and Fuel Flow, as shown in Fig. 1.

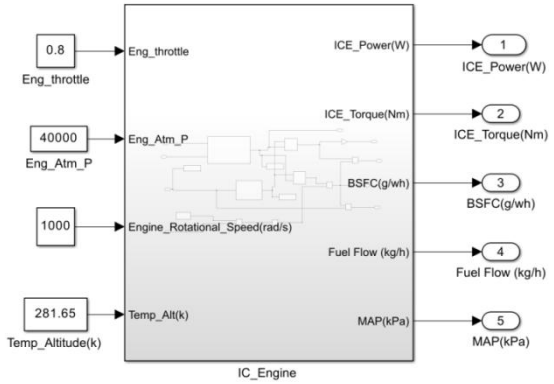

Fig. 1. ICE Simulink model with inputs and outputs

Figure 2 shows the inside view of the Simulink model. The engine Manifold Air Pressure (MAP) is calculated from the model as:

$$P_{ma} = P_{min} + \left(\frac{P_{atm}}{1000}\right) \times \eta_{th} \quad (1)$$

where: P_{atm} is the engine atmospheric pressure (Pa), P_{min} is the minimum atmospheric pressure (Pa) η_{th} is the engine throttle.

The engine Fuel Flow (FF) and ICE power (P_{ICE}) are determined from the engine rotational speed and Manifold Air Pressure (MAP) by interpolation with a 2-D lookup in Simulink using ICE data. The ICE data used to create the lookup is shown in Tables 1 and 2, respectively. An altitude-correction factor has also been included in the model to determine the ICE power at various altitudes during flight. It determines the ICE power at any given altitude from the temperature at sea level, the temperature when the UAV is in flight, and the ICE Power from the lookup table as [11]:

$$P_{ICE,Alt} = P_{ICE}\sqrt{\frac{T_{alt}}{T_{sea\_level}}} \quad (2)$$

where: T_{sea_level} is the temperature at sea-level in Kelvin (K), T_{alt} is the temperature at a given altitude in Kelvin (K), P_{ICE} is the ICE power in Watts (W), $P_{ICE,Alt}$ is the ICE power at a given altitude in Watts (W), FF is the engine fuel flow in (kg/h).

An atmosphere model was also created using a 2-Look-up table based on the International Standard Atmosphere (ISA), from which the temperature at any given altitude could be determined from the UAV's altitude. This is shown in Fig. 3. The engine Brake Specific Fuel Consumption (BSFC) is obtained from the engine ICE power and Fuel flow as:

$$BSFC = \frac{FF}{P_{ICE,Alt}} \quad (3)$$

The engine torque is determined from the ICE power and engine rotational speed as:

$$T_{ICE} = \frac{P_{ICE,Alt}}{\omega} \quad (4)$$

where T_{ICE} is the engine torque in N, ω is the engine rotational speed in rad/s.

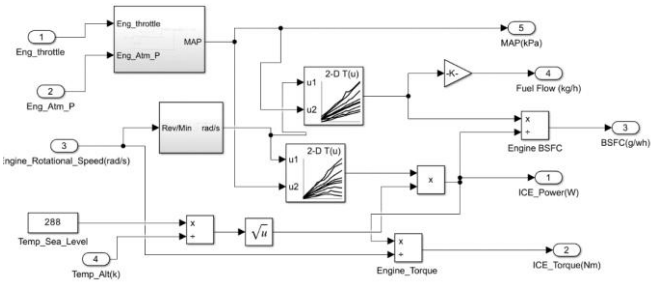

Fig. 2. Structure of the ICE Simulink model with input and output signals

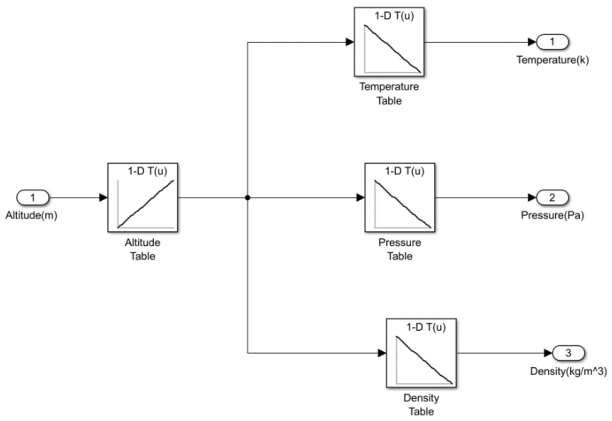

Fig. 3. Atmospheric model based on altitude input

Table 1. ICE power [W] at various engine speeds and MAP values

n [rpm]	MAP								
	60	70	80	90	92	94	96	98	100
1500	18.85	47.12	65.97	67.54	69.12	67.54	67.54	69.12	86.39
2100	59.38	98.96	127.55	149.54	151.74	160.54	178.13	200.12	224.31
2800	93.83	149.54	187.66	237.50	249.23	255.10	307.88	366.52	398.77
3500	109.96	161.27	245.57	307.88	326.20	351.86	421.50	591.14	531.45
4500	164.93	245.04	339.29	438.25	447.68	494.80	565.49	673.84	772.83
5100	181.58	245.67	389.87	496.69	528.73	571.46	662.25	822.47	993.37
5500	184.31	293.74	403.17	535.64	570.20	622.04	748.75	956.09	1059.80
6000	163.36	276.46	420.97	565.49	609.47	691.15	860.80	1131.00	1193.80
7000	124.62	249.23	417.83	586.43	645.07	762.36	996.93	1246.20	1429.40

Table 2. Fuel flow rate [g/h] at various engine speeds and MAP values

n [rpm]	SMAP								
	60	70	80	90	92	94	96	98	100
1500	31	32	46	53	55	57	65	73	82
2100	40	44	54	69	74	80	92	103	111
2800	50	63	69	74	95	98	126	145	153
3500	66	75	87	110	117	127	150	175	190
4500	83	98	115	143	148	162	191	232	246
5100	93	102	130	159	167	182	208	260	310
5500	100	118	137	169	178	190	232	287	313
6000	104	126	151	184	191	206	253	326	337
7000	123	144	174	210	217	244	321	400	408

3. Results and discussion

3.1. Model output results at various engine throttle positions

This section discusses the results obtained from the model, with the validation of the model output results obtained by previous authors. This is explained in the relevant sub-sections below.

The model was run to evaluate the effect of increasing the engine throttle on the various outputs of the model by setting the engine throttle to zero when the engine is idle to full throttle when the engine draws maximum air fuel into the combustion chamber of the engine, as shown in Fig. 4–7. The results of each output are explained in the relevant subsections below.

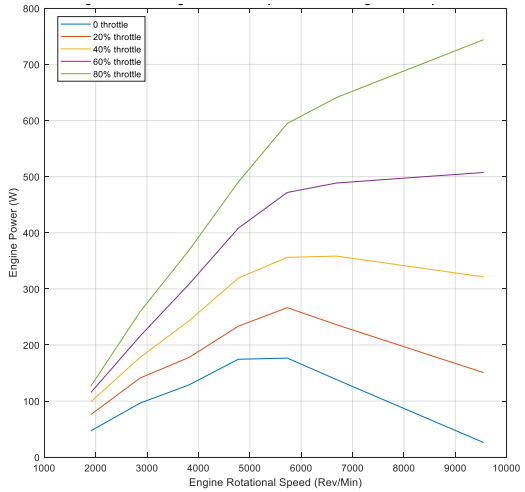

Fig. 4. Engine power against engine rotational speed at various engine throttle positions

Engine power at various throttle positions

The engine power curves increase as the throttle is increased from 0% to 80%, with the lowest power at 0% and the highest at 80%, as shown in Fig. 4.

Engine torque at various throttle positions

A similar trend is also observed in the engine torque curves, which increase as the throttle is increased from 0% to 80%, as shown in Fig. 5.

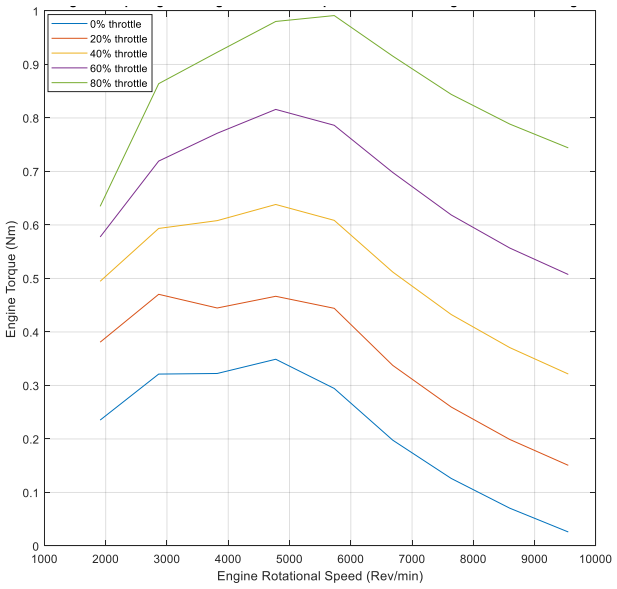

Fig. 5. Engine torque against engine rotational speed at various engine throttle positions

Engine fuel flow at various throttle positions

The engine fuel flow curves rise as the engine throttle is increased from 0% to 80%, with the lowest fuel flow at 0% throttle and the highest at 80% throttle, as shown in Fig. 6.

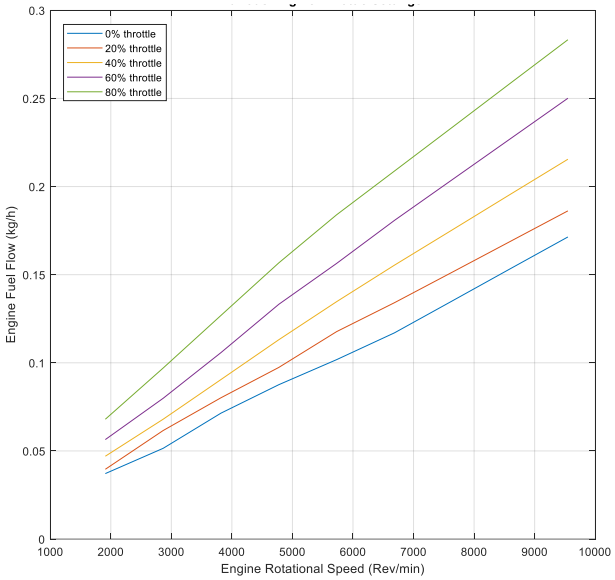

Fig. 6. Engine fuel flow against engine rotational speed at various throttle positions

Engine brake specific fuel consumption at various throttle positions

The engine brake-specific fuel consumption curves, on the other hand, decrease as more throttle is added to the engine i.e. as the engine throttle increases from 20% to 80%, with the highest brake-specific fuel consumption curve at 20% throttle and the lowest brake-specific fuel consumption curve at 80%, as shown in Fig. 7.

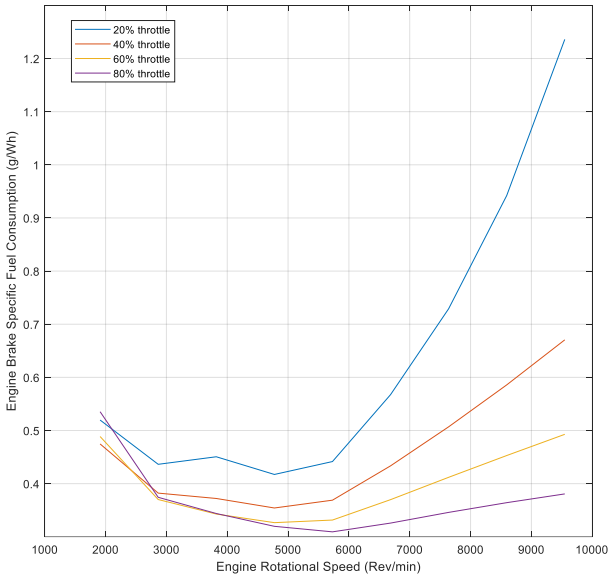

Fig. 7. Engine brake specific fuel consumption against engine rotational speed at various throttle positions

3.2. Model results and comparison

A comparison between model results and those of previous researchers experiments was conducted, as real engine data from a manufacturer could not be obtained for the developed model. 8 papers from the literature were used for comparison. Figures 8–11 show the modeled results, which were compared with those of previous researchers. This is explained in the relevant sub-sections below.

Engine power comparison

Figure 8 shows the engine power curves obtained from the model, which were compared with results from previous authors' experiments on ICEs [2, 7, 17]. It can be observed that the simulated engine power curves closely predict the power curves obtained from experiments since they both follow the same increasing trend pattern, where the engine brake power increases with increased engine rotational speed, with maximum power attained at a specific rpm value (8200 rpm, 693 W for the simulated power curve). A discrepancy is observed at various engine rotational speeds. The main reason for the discrepancy is that the modeled ICE was fitted with power curves obtained experimentally by previous researchers from the literature for different-sized ICE (between 30 kW and 40 kW). In contrast, the modeled ICE has a maximum power of only 700 W. Proper validation could only be achieved if the author could obtain engine performance curves from the manufacturer for the modeled ICE. However, a deviation always exists between the modeled ICE and the experimentally obtained ICE. The deviation is mainly due to the fact that the actual combustion process is a complex phenomenon, and simulations from a developed model are not sufficiently sophisticated to account for the factors that occur during the actual combustion process [7].

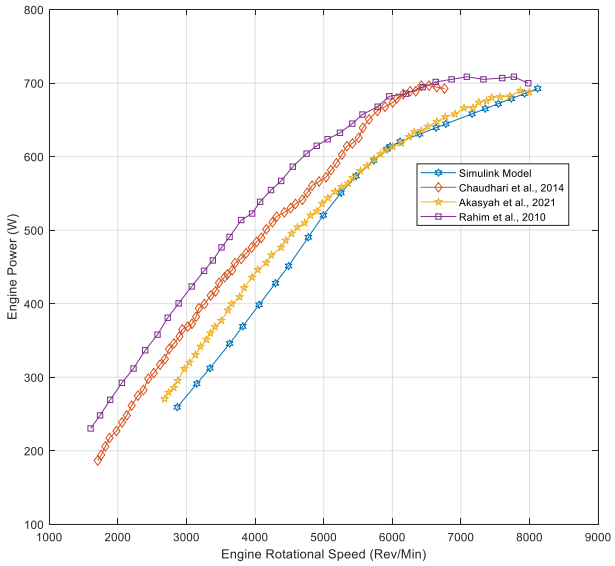

Fig. 8. Engine power vs engine rotational speed validation

Engine torque comparison

Figure 9 shows the engine torque results from the model, which were compared with engine torque curves obtained by previous authors experimentally. The simulated engine torque curves increases with increased rotational speed to a maximum value (0.35 Nm, 4800 rpm), which represents the maximum operating torque of the engine, and then decrease again as the engine speed is further increased.

The experimental engine torque curves obtained by previous authors [7, 15, 17] also show the same predictions, where it increases to a maximum operating point and decreases when the engine rotational speed is further increased, as shown in Fig. 9.

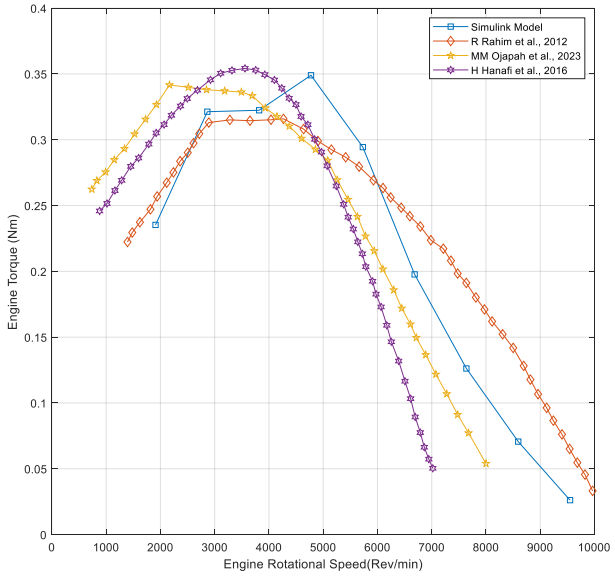

Fig. 9. Engine torque vs engine rotational speed validation

A discrepancy is also observed between the modelled engine torque curves and experimental torque curves obtained by researchers due to the same reason stated in previous section.

Brake specific fuel consumption comparison

Figure 10 shows the simulated BSFC obtained from the developed model, along with experimental BSFC curves from previous authors [2, 10, 17].

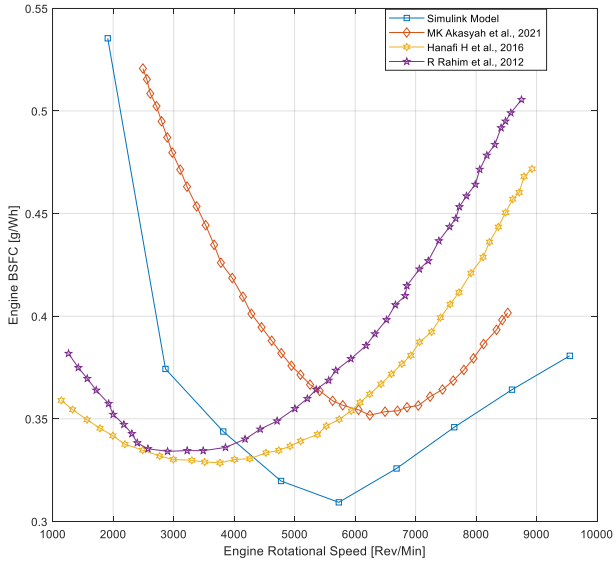

Fig. 10. Engine brake specific fuel consumption vs engine rotational speed validation

Both the simulated curve and the experimental curves follow the same trend: the engine BSFC decreases with increasing rotational speed to a minimum value, which represents the maximum operating point of the engine, and then increases again as the rotational speed is further increased. A discrepancy is also observed between the modeled BSFC curves and the experimental BSFC curves reported by previous researchers, for the same reasons stated in the previous section.

Engine fuel flow comparison

Figure 11 shows the model output for engine fuel flow, compared with experimental curves for engine fuel flow obtained by previous authors for ICEs [21]. The simulated fuel flow curves closely approximate the experimental curves, as they all show an increase in fuel flow with increasing rotational speed. A deviation is also obtained between the engine fuel flow curves obtained from simulation and those obtained experimentally due to the same reasons stated in the previous section.

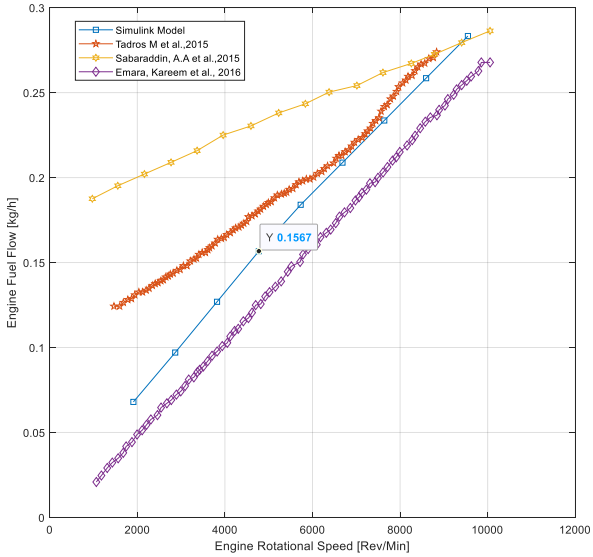

Fig. 11. Engine fuel flow vs engine rotational speed validation

3.3. Engine contour maps

An engine contour showing the engine's relative operating point was obtained from the model, as shown in Fig. 12. At this time, the contour map is static. More research would be conducted on how to make the map dynamic during simulation.

4. Conclusion

This paper provides a unique modelling approach of an ICE for a UAV given some input parameters to the model. The model results were compared with those of previous researchers' experimental results. Both the model results and the experimental results agreed, as they showed the same curve. The Novelty in the modelling approach used in this article can be summarized as follows:

– The ICE model has been developed so it can be used as a drive component for UAV propulsion.
– The developed model allows the ICE to estimate power, torque, Fuel Flow, and BSFC at various temperatures, pressures, and altitudes during the flight of the UAV, unlike ground vehicles, where there are no pressure or altitude variations.

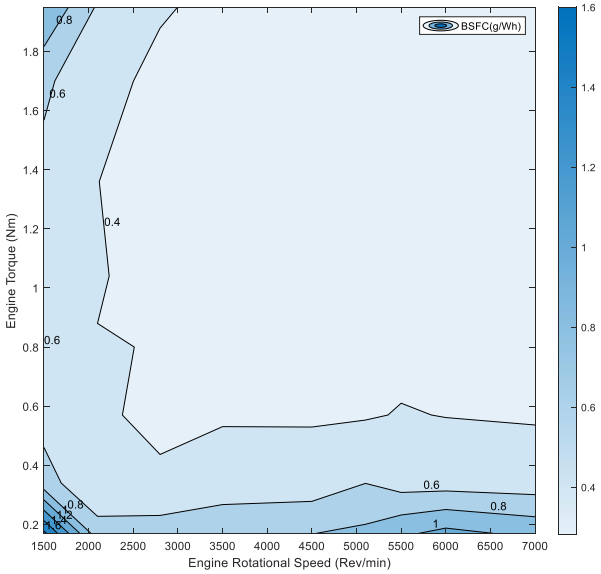

Fig. 12. Engine fuel map with BSFC contours using ICE data

It should be noted that the model has the following limitations:

- The model is limited to Combustion engines suitable for small UAVs, as it can only produce a maximum power of 700 W
- The model is only operational between 1000 rev/min and 10000 rev/min.

The following research directions could be explored from the present study:

- Integrating the developed model into a UAV powertrain to evaluate its functionality in simulation
- Performing an experimental setup to validate the developed model with experimental data of UAV engines from a manufacturer
- Developing scaling laws suitable for UAV combustion engines that could boost the engine power beyond 700 W.

Nomenclature

BSFC	brake specific fuel consumption
FF	engine fuel flow
ICE	internal combustion engine
ISA	international standard atmosphere
MAP	manifold air pressure
P_{atm}	engine atmospheric pressure
P_{ICE}	engine power
$P_{ICE,Alt}$	ICE power at a given altitude
P_{ma}	engine manifold air pressure
P_{min}	minimum engine atmospheric pressure
T_{alt}	temperature at a given altitude
T_{ICE}	engine torque
T_{sea_level}	temperature at sea level
UAV	unmanned aerial vehicle
ω	engine rotational speed
η_{th}	engine throttle

Bibliography

[1] Al-Atabi MT, Yusaf TF. Experimental investigation of a single cylinder diesel engine as a hybrid power unit for a series hybrid electric vehicle. Student Conference on Research and Development. IEEE. 2002:261-264. https://doi.org/10.1109/SCORED.2002.1033107

[2] Akasyah MK, Yusri IM, Mamat R, Jamlos MF, Abdul Majeed AP. Experimental evaluation of tertiary blends of water in diesel with butyl alcohol using compression ignition engine. IOP Conf Ser: Mater Sci Eng. 2021;1092:012072. https://doi.org/10.1088/1757-899X/1092/1/012072

[3] Ammad ud Din S, Zhuge W, Song P, Zhang Y. A method of turbocharger design optimization for a diesel engine with exhaust gas recirculation. P I Mech Eng D-J Aut. 2019;233(10): 2572-2584. https://doi.org/10.1177/0954407018802560

[4] Boretti AA. Numerical evaluation of the performance of a compression ignition CNG engine for heavy duty trucks with an optimum speed power turbine. Int J Eng Technol Innov. 2011;1(1):12-26. https://ojs.imeti.org/index.php/IJETI/article/view/4

[5] Chen S, Ma C, Zhang H, Xu C, Lei F, Feng T et al. Engine performance improvements through turbocharger matching and turbine design. Energy Sci Eng. 2022;10:3384-3396. https://doi.org/10.1002/ese3.1225

[6] Chen T, Zhuge W, Zheng X, Zhang Y, He Y. Turbocharger design for a 1.8 liter turbocharged gasoline engine using an integrated method. Turbo Expo: Power for Land, Sea, and Air 2009;48883:589-598. https://doi.org/10.1115/GT2009-59951

[7] Chaudhari AJ, Sahoo N, Kulkarni V. Simulation models for spark ignition engine: a comparative performance study. Energy Procedia. 2014;54:330-41. https://doi.org/10.1016/j.egypro.2014.07.276

[8] Dresler P, Richtář M. Simulation model of the single cylinder combustion engine MZ125. Perner's Contacts. 2011;6(4):80-88. https://ojs.upce.cz/index.php/perner/article/view/900

[9] El Hameur MA, Sehili Y, Cerdoun M, Tarabet L, Ferrara G. An approach to select an appropriate turbocharger for matching with an internal combustion engine. Int J Engine Res. 2023;24(5):2072-2090. https://doi.org/10.1177/14680874221108581

[10] Hanafi H, Hasan MM, Rahman MM, Noor MM, Kadirgama K, Ramasamy D. Numerical modeling on homogeneous charge compression ignition combustion engine fueled by diesel-ethanol blends. MATEC Web Conf. 2016;74:00037. https://doi.org/10.1051/matecconf/20167400037

[11] Hung JY, Gonzalez LF. On parallel hybrid-electric propulsion system for unmanned aerial vehicles. Prog Aerosp Sci. 2012; 51:1-17. https://doi.org/10.1016/j.paerosci.2011.12.001

[12] Kang YS, Lim BJ, Cha BJ. Multi-stage turbocharger system analysis method for high altitude UAV engine. J Mech Sci Technol. 2017;31(6):2803-2811. https://doi.org/10.1007/s12206-017-0523-4

[13] Kravchenko S, Obodets D, Kuzmenko A. Improving the energy efficiency of a two-stroke engine with crankcase scavenging for UAVs by implementing an electronic fuel injection

system. Combustion Engines. 2026;204(1):72-80. https://doi.org/10.19206/CE-213457
[14] Magdas VB, Mastan DC, Burnete N. Simulation possibilities of the internal combustion engine management elements using Lotus Engine Simulation software. IOP Conf Ser: Mater Sci Eng. 2020;997(1):012121. https://doi.org/10.1088/1757-899X/997/1/012121
[15] Ojapah MM, Diemuodeke EO. Effect of palm oil biodiesel blends on engine emission and performance characteristics in an internal combustion engine. Open J Energy Effic. 2023; 12(1):13-24. https://doi.org/10.4236/ojee.2023.121002
[16] Ramkumar J, Krishnasamy A, Ramesh A. A novel method to overcome the shortcomings of turbocharging a single cylinder diesel engine. Int J Engine Res. 2023;24(3):873-887. https://doi.org/10.1177/14680874211066744
[17] Rahim R, Mamat R, Taib MY, Abdullah AA. Influence of fuel temperature on a diesel engine performance operating with biodiesel blended. J Mech Eng Sci. 2012;2:226-236. https://doi.org/10.15282/jmes.2.2012.10.0021
[18] Shanmuganathan U, Govarthanan R, Muthumailvaganan A, Imayakumar A. Modeling and dynamic simulation of IC engine driven permanent magnet generator using Matlab/Simulink for hybrid tracked vehicle. IEEE Conference on Electric and Hybrid Vehicles. 2006:1-6. https://doi.org/10.1109/ICEHV.2006.352289
[19] Stewart P, Gladwin D, Stewart J, Cowley R. Generator voltage stabilisation for series-hybrid electric vehicles. IFAC Proc Vol. 2007;40(23):222-228. https://doi.org/10.1016/S1474-6670(17)69270-X
[20] Stevenson JD, Long D, Maslanik J, O'Young S. Integration of a miniature synthetic aperture radar (MicroSAR) on the aerosonde UAV. https://www.academia.edu/98529427/Integration_of_a_Miniature_Synthetic_Aperture_Radar_MicroSAR_on_the_Aerosonde_UAV
[21] Tadros M, Ventura M, Guedes Soares C. Numerical simulation of a two-stroke marine diesel engine. Towards Green Marine Technology and Transport. Taylor & Francis Group, London. 2015:609-617. https://www.taylorfrancis.com/chapters/edit/10.1201/b18855-82/numerical-simulation-two-stroke-marine-diesel-engine-tadros-ventura-guedes-soares
[22] Wróblewski P, Bratkowski P, Borcuch D, Kiszkowiak Ł. Prototype station dedicated to aircraft engine propeller profiles and advanced materials testing. Combustion Engines. 2025;201(2):165-175. https://doi.org/10.19206/CE-204319
[23] Yixuan WA, Yan SH, Maolin CA, Weiqing XU, Qihui YU. Efficiency optimized fuel supply strategy of aircraft engine based on air-fuel ratio control. Chin J Aeronaut. 2019;32(2): 489-498. https://doi.org/10.1016/j.cja.2018.10.002

Lionel Dongmo Fouellefack, DEng. – Department of Smart and Systems Engineering, University of South Africa, South Africa.
e-mail: *25201662@mylife.unisa.ac.za*

Prof. Sumbwanyambe Mbuyu, DEng. – Department of Smart and Systems Engineering, University of South Africa, South Africa.
e-mail: *sumbwm@unisa.ac.za*

Prof. Etienne Alain Feukeu, DSc., DEng. – Department of Smart and Systems Engineering, University of South Africa, South Africa.
e-mail: *efeukeea@unisa.ac.za*

Prof. Dhlamini Mokhotjwa, DSc., DEng. – Department of Physics, University of South Africa, South Africa.
e-mail: *dhlamms@unisa.ac.za*